J Appl Electrochem (2013) 43:209–215
DOI 10.1007/s10800-012-0484-3

ORIGINAL PAPER

Emission spectra and transient photovoltage in dye-sensitized solar cells under stress tests

M. Giustini · D. Angelone · M. Parente · D. Dini · F. Decker · A. Lanuti · A. Reale · T. Brown · A. di Carlo

Received: 24 July 2012 / Accepted: 21 September 2012 / Published online: 6 October 2012

Abstract Dye-sensitized solar cells have been tested before, during, and after stress tests performed either under intense Xe-lamp illumination (equivalent to 1 sun up to 2.5 sun) or under thermal cycles between room T and 80 °C. In-situ emission spectra and transient photovoltage decay curves have been taken to monitor the cell aging conditions. Incipient degradation phenomena in aged cells can be detected by changes in emission intensity, maximum photovoltage and in the time constant of photovoltage decay. UV-filtering of the Xe beam can prevent such cell degradation, provided the cell overheating is avoided.

Keywords Dye-sensitized solar cell (DSC) · Solar energy conversion · Sensitizer emission · Photovoltage transients · Aging · Accelerated tests

Electronic supplementary material The online version of this article (doi:10.1007/s10800-012-0484-3) contains supplementary material, which is available to authorized users.

M. Giustini (✉) · D. Angelone · M. Parente · D. Dini · F. Decker (✉)
Department of Chemistry, University of Roma "La Sapienza", P.le Aldo Moro 5, 00185 Rome, Italy
e-mail: mauro.giustini@uniroma1.it

F. Decker
e-mail: franco.decker@uniroma1.it

M. Giustini
CSGI c/o Department of Chemistry, University of Bari, Via Orabona, Bari, Italy

A. Lanuti · A. Reale · T. Brown · A. di Carlo
Department of Electronic Engineering, CHOSE–Centre for Hybrid and Organic Solar Energy, University of Rome Tor Vergata, Viale Politecnico 1, 00133 Rome, Italy

1 Introduction

The stability of dye-sensitized solar cells (DSCs) [1] in operating conditions represents a critical issue for the commercialization of this low-cost technology for solar energy conversion [2]. In fact, the sole attainment of record conversion efficiencies of more than 10 % [3–6] can turn into a barely satisfactory achievement if such performances are not accompanied by long-term reproducibility and device durability [7–11]. Several reasons for the degradation of DSCs performance have been addressed depending on the type of applied stress, i.e., if thermal stress [12–15]—irradiation [16–18], in particular, depending on DSC placement (indoor/outdoor). The analyses took into account mainly the procedure of cell assembly/encapsulation [19, 20] and, more importantly, the chemical nature of the various components (photoelectrode, dye, redox shuttle, and electrolyte) [21] of the DSCs under examination in real-time or accelerated tests [7–11, 22]. For these reasons, it appears crucial, although quite complicated, to define suitable conditions of artificial aging according to universally accepted standards [23, 24], or to choose a time window wide enough to be of practical significance in the analysis of the outdoor DSC performance [25] when unambiguous information on the actual long-term stability of these devices is required. In addition to this, it is also of paramount importance to identify appropriate chemical/physical parameters that have to be analyzed in conjunction with the temporal recording of the paradigmatic DSC quantities [short-circuit current density (J_{sc}), open-circuit potential (V_{OC}), fill factor (FF), and overall efficiency (η)] for assessing the causes of DSC performance degradation under the adopted conditions of stress [2]. In this regard, in-situ techniques, based on the determination of optical and

electrical parameters, like electrochemical impedance spectroscopy (EIS) [26, 27], intensity-modulated photocurrent spectroscopy (IMPS) [28], and intensity-modulated photovoltage spectroscopy (IMVS) [29] have been profitably used for the study of the aging mechanisms that act on DSCs. Other spectroscopic and imaging techniques like IR [30], UV–Vis [31], and spatially resolved mapping of photocurrent [32] have been also used as complementary methods together with transient absorption techniques [33]. The study of the emission properties of DSCs upon excitation of the cell is here proposed for the analysis of degradation mechanisms in DSCs together with the analysis of photovoltage transients [34]. Photoluminescence (in the steady state) studies have been used in the past to characterize semiconductor nanoparticles [35, 36], but only seldom were they reported for sealed DSCs [37, 38]. Regarding the luminescence properties of Ru-based dyes, very recently a thorough investigation based on femto-seconds fluorescence spectroscopy has been presented [39]. This study reveals a very complex energy landscape of the excited states of N719 both in solution and when adsorbed over several semiconductors. Upon excitation at 400 nm, the emission that peaked around 730 nm is not ascribable to a fluorescence decay but to phosphorescence (though the band presents all the features of a fluorescence signal, e.g., mirror-like shape with respect to the absorption band; nanoseconds lifetimes). The reason lies in the extremely fast intersystem crossing (fs timescale) from the first singlet excited state that leads to the population of the first excited triplet state from where radiative relaxation to the ground state occurs (phosphorescence). The real fluorescence signal is peaked around 550 nm and has a very low quantum yield and extremely short lifetime ($\leq$30 fs) [40] and cannot be detected in the experiments on intact DSCs here presented. In fact, the strong absorption of the I_3^-/I_2 redox couple prevents the use of excitation wavelength below 500 nm, and therefore the fluorescence signal lies outside the detected region. Anyhow, as the photoelectron injection into the TiO_2 substrate mainly occurs from the first excited triplet state [39], the measurements of the photo emission around 730 nm represent the most significant parameter to be measured as it is directly relatable to the DSC performances under different aging conditions here explored. Our combined study represents one of the few for this kind of investigations. In the present study, we demonstrate that, through the measurement of dye emission, it is possible to follow the chemical stability of the molecules of sensitizer and associate it to the electrical behavior of the whole DSC. The performances of DSCs based on TiO_2 photoanodes have been analyzed after thermal and optical stress tests that mimic the actual operating conditions of DSCs under sunshine.

2 Experimental part

2.1 TiO_2 cells' preparation

Dye-sensistized photoanodes were prepared via Doctor Blade® technique, using a slurry paste made of P25® Degussa TiO_2 nanopowders (25-nm nanoparticle size) deposited on F:SnO_2-coated glass (FTO glass) and then annealed at 450 °C for 30 min. The resulting mesoporous thin film was then dipped in an ethanolic solution 5 mM of N719 [*cis*-bis(isothiocyanato)-bis(2,2′-bipyridyl-4,4′-dicarboxylato)-ruthenium(II)bis-tetrabutylammonium] for 24 h. Afterward, the sensitized electrodes were rinsed in anhydrous ethanol and dried under soft nitrogen flux. The counter electrode consists of a platinized FTO glass sprayed with Platisol T® (from Solaronix) solution and then annealed at 400 °C for 5 min. Successively, the sensitized photoanode and the platinized electrode were sandwiched using a Surlyn® thermo-sealant polymer film, about 60 μm thick, acting as both spacer and sealant. Finally, a solution of electrolyte Iodolyte Z-150 (from Solaronix) was introduced through a predrilled hole on the counter-electrode using the vacuum back-filling technique. The hole was sealed with a glass piece of the proper size and Surlyn® as well. The geometric area of the electroactive part of the DSC constructed with this method is 0.7 cm × 0.7 cm. The three cells used for the aging under irradiation have been prepared on the same substrate, as shown in Fig. 1. This allowed us to compare the effect of different light soaking experiments on the DSCs, starting from very similar initial condition for each of the three cells. A single DSC of the same batch, however, has been prepared on a separate substrate to perform only the thermal stress experiments on it (from ambient to 80 °C, and back after a well-defined heating time interval).

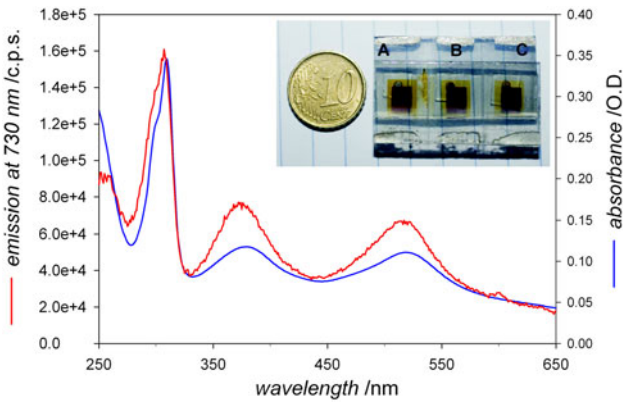

Fig. 1 Absorption (*blue line*) and excitation (*red line*) spectra of a 0.11 mM N719 solution in anhydrous ethanol. The *inset* shows the tris of DSCs (CD41) used for the aging experiments described in the text (named A, B and C, from *left* to *right*). (Color figure online)

2.2 Measurements and equipment

Electrochemical measurements were performed using an Autolab potentiostat PGSTAT-12 Echo Chemie BV. Spectroscopic measurements were carried out using a spectrofluorimeter FLUOROMAX-2, Jobin–Yvon-Spex and a spectrophotometer Cary 50 (from Varian-Agilent Technologies). All the emission spectra have been recorded in the range of 600–900 nm with $\lambda_{exc} = 520$ nm. To ascertain that such spectra are related to the photoexcitation of the N719 dye molecules, an excitation spectrum (detection set at 730 nm; Hellma fluorescence quartz cuvette, 1 cm × 1 cm) and an UV–Vis absorbance of the same liquid sample containing the dye have been taken (Hellma quartz cuvette, 1 cm), and are shown in Fig. 1. In-situ photo-emission measurements were performed using a homemade sample holder equipped with micrometric adjustable position for each of the three axes plus a goniometric table allowing the precise and reproducible orientation of the DSC surface (colored electrode back) with respect to the impinging excitation beam (see Electronic Supplementary Information–ESI). Spectra were acquired with a resolution of 1 nm, with both excitation and emission slits set at 5 nm. The utmost care was paid to avoid direct reflection of the measuring beam from reaching the spectrofluorometer photomultiplier. In the case of photopotential versus time measurements, the DSCs were excited with a frequency-doubled Nd:YAG pulsed laser ($\lambda_{em} = 532$ nm Quanta System, Handy 710), with a pulse energy of 0.3 J and a pulse width of 7 ns. Laser pulses were delivered to the DSCs by means of an optical fiber (Oriel) located at a distance of 1 cm from the photoanode. The data acquisition was performed by means of the DAQ board PCI-6013 (National Instruments) directly connected to the DSC via the shielded connector block BNC-2120 (National Instruments). A home-built acquisition program developed under LabView environment took care of the data acquisition, signal averaging (when required), and storage of the measurements. Depending on the measurement, data acquisition rates were 1,000 and 200,000 pts s^{-1} for the recording of the whole discharge process of the DSC and of the initial rising part of photopotential, respectively. Data were analyzed and handled with the software SigmaPlot 10.0.1 (Systat-Software). Irradiance was measured with a radiometer SOLAR118 from Instrument Messgeräte. Experiments under controlled thermal and optical stress were performed using different resistive circuits in series (100 Ω, 450 Ω, and open- and short-circuits) under natural light (in summer) and under Xe lamp at different irradiance values using a water cuvette for the filtering of hot IR radiations, and, optionally, a 400-nm high-pass filter (Baird Atomics BA400). Cycles of thermal stress were performed using a heater tube (Büchi TO-50) at 80 °C when the cell was in the open-circuit status.

3 Results

All the cells measured in this article have been first activated by repeatedly cycling under UV-filtered, AM 1.5 light, and then submitted either to thermal, or to irradiation stress tests. In Fig. 2a, the photoluminescence spectra of the dye–cell submitted to thermal stress at 80 °C in the dark, for consecutive time intervals, are shown. A moderate

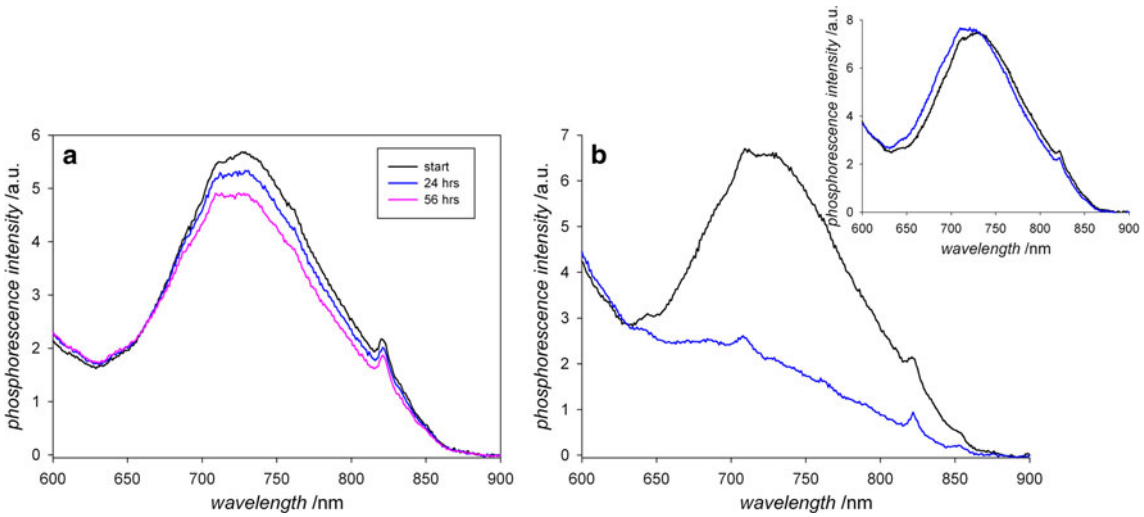

Fig. 2 Emission spectra of activated DSCs under different aging conditions. **a** Thermal stress effects detected by incubating the DSC at 80 °C for the time indicated in the legend. **b** The effects of 27-h exposure to 2.5 sun Xe lamp not filtered for the UV component (cell C) and, in the *inset*, the spectra obtained by filtering the incident Xe light with a BA-400 filter (cell B). For the sake of clarity, only two spectra for each DSC are shown. *Black line* start; *blue line* after 42-h exposure. (Color figure online)

decrease of the peak intensity, proportional to the total time the cell has been kept at higher T, has been observed. The three DSC cells of the tris CD-41 have been used for the irradiation stress tests, after assessment of their similar photoresponse when illuminated. Cell A was taken as the reference cell, without further aging; cell B was kept under the UV-filtered white light beam from the Xe lamp; and cell C was aged under the same light beam, but without any UV filter in the optical path. Cell A, cell B, and cell C have been periodically measured in the spectrofluorimeter, and their photopotential transients have been measured at the beginning and at the end of the aging tests. In Fig. 2b, one can see how the phosphorescence spectrum of a DSC looks like—before, and after the irradiation tests. When the spectrum used for irradiation contained an important UV component (cell C), the emission peak at 720 nm collapsed already after 6 h, and almost disappeared after 27 h of irradiation with the intensity set at 2.5 sun to literally vanish after 42 h of exposure (Fig. 2b, blue line). However, by filtering off the UV component, the measured phosphorescence spectrum remained practically unchanged (see spectra from cell B in the inset of Fig. 2b), except for a slight blue-shift of the emission peak that could be related to minor modification of the N719 dye due to partial substitution of the –SCN groups by water or solvent molecules [31]. Such tests on cell B (no UV) have been initially taken under a light intensity of 1 sun and in open circuit then, at different points of the power curve, by applying various load resistors ($450 \leq R \leq 100\ \Omega$), because the aging with a photocurrent crossing the cell is more severe than that under open circuit. For the last 20 h of this test under a light intensity of 2.5 sun, a load resistor of 100 Ω was applied: still, no significant changes of the phosphorescence peak shape and intensity have been noticed.

About the power characteristics of the stressed DSCs summarized in Fig. 3, some features are worth of mentioning. The first heat treatment has a positive effect on the short-circuit current and on the fill factor (Fig. 3a), showing that this treatment has activated again the cell and has reduced the overall series resistance. The second heat stress test, on the other hand, has a depressing effect on the *I* versus *V* cell characteristics. The open-circuit potential is the only cell parameter that decreases from the first thermal stress test onward. Within the tris of cells aged under Xe lamp beam, the *I* versus *V* plot of the cell C changed significantly more than that of all other cells (Fig. 3b), with respect to the short-circuit current and the open-circuit voltage. First, the cell power output greatly increased after exposure to light during the initial 6–11 h, in particular because of a growing short-circuit current; later, however, the cell current started to decline, and so did its conversion efficiency. The only parameter always decreasing during this aging test, and that too at a steep rate, has been the cell

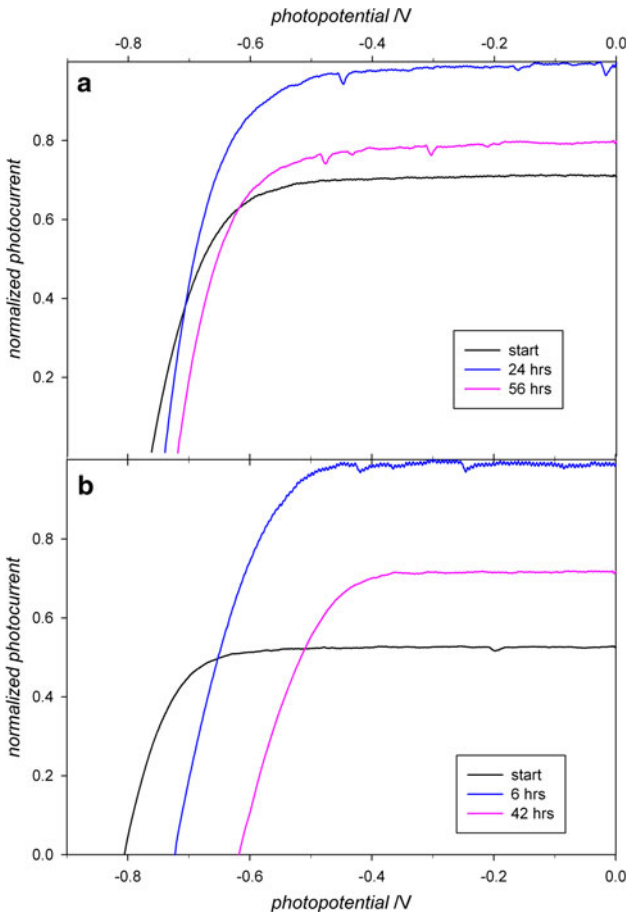

Fig. 3 Normalized I versus V curves for activated DSCs under different aging conditions, taken under a 100 mW cm^{-2}, UV-filtered white light beam from a Xe lamp. Typical value of short-circuit photocurrent after activation for every cell of CD41 (at AM 1.5 simulated sunlight) was 8 mA cm^{-2}. Potential scan rate, 10 mV s^{-1}. **a** Thermal stress effects detected by incubating the DSC at 80 °C for the time indicated in the legend. **b** Effects of the exposure to the 2.5 sun Xe lamp not filtered for the UV component for the time indicated in the legend

open-circuit potential. Finally, for the cell B, after an initial efficiency increase, a substantially stable *I* versus *V* curve has been recorded (data not shown).

The comparison of transient photopotential experiments between the aged cell C and of the reference cell A is presented in Fig. 4. In the 1 μs–10 ms range, the photopotential rose to a value close to 0.8 V in about 1 ms for cell A, whereas it reached its maximum value of 0.6 V in 0.4 ms for the aged cell C (Fig. 4a). Upon acquiring the whole decay curves (0.1 ms–10 s range), further differences among the two cells appear (Fig. 4b). Both decay curves show at least two different slopes, one shallower in the beginning and another a steeper one in the last part of the curve. In this last part (consisting of photopotentials lower than 0.1 V), a displacement of about 10 s between the two curves is evident (see the horizontal arrow in

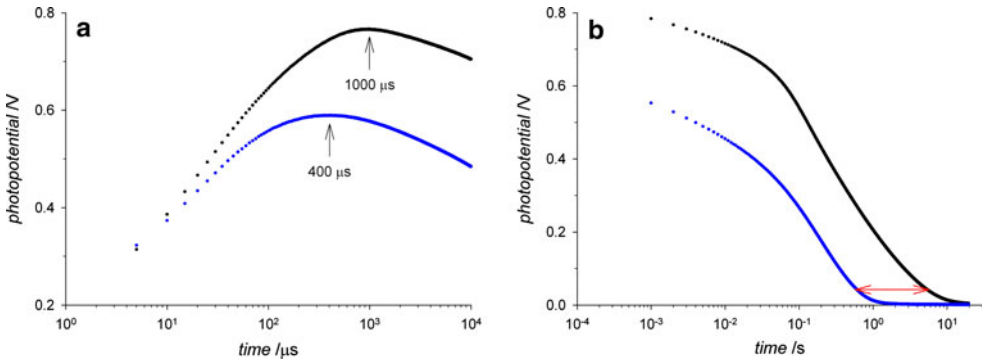

Fig. 4 Photopotential rise (**a**) and decay (**b**) curves for activated CD41 A (*black line*) and C (*blue line*). The shifts in both the time at which the maximum V_{OC} is attained (**a**) and in the recovery of the dark-adapted photopotential (**b**) are marked. See ESI for further details. (Color figure online)

Fig. 4b). The UV-aged C cell showed the faster photovoltage decay; the reference A cell had an overall decay time ten times longer than that of the UV-aged cell.

4 Discussion

It is well known that stressed DSCs first show an improvement in their power characteristics followed by a decay leading to an irreversible degradation with a significant loss of power conversion efficiency. This temporary improvement in DSC performances has been attributed to electrode activation because of thermal desorption of impurities, UV-induced degradation of organic contaminants or UV-induced necking between TiO_2 nanoparticles, among other effects [41]. On the contrary, the phosphorescence peak intensity from our cells never increased, either after thermal or irradiation stresses. Such a signal originates from anchored dye molecules that upon excitation dissipate the excess energy in a radiative way with no consequent charge injection into the supporting electrode. Very likely, the origin of such a behavior is related to the existence of a fraction of dye molecules not chemically bound to the substrate but merely physisorbed onto it or onto the FTO, as it has been shown that N719 molecules linked to a TiO_2 substrate do not emit [39]. To a lesser extent, dye molecules dissolved in the electrolyte can also contribute to the observed luminescence.

Let us discuss separately the aging effects due to thermal stress applied at 80 °C in the dark from that due to irradiation. Thermal stress has led to a slow but monotonic decrease in the cell fluorescence intensity. This is a strong clue of ongoing, progressive, thermally activated dye degradation. As stated before, as the phosphorescence detected in intact DSCs is mainly ascribable to those dye molecules, which are not chemically linked to the semiconductor substrate and do not inject electrons into TiO_2, this suggests that light-emitting molecules are more sensitive to the degradation phenomena induced by an increase of temperature. The thermal activation of a process of dye degradation due to the chemical attack of the redox shuttle [I_2 is a mild oxidant: $E°$ (I_2/I^-) = 0.29 V *vs* SHE in ACN and $E°$ (I_2/I^-) = 0.54 V *vs* SHE in water] [42] could be another cause of the observed decrease of the emitted light. In its initial stage, such a thermal degradation of the emission is limited to the physisorbed dye or to dye molecules in solution. This is because, in the same time period, the power output of the cell grew up (Fig. 3a). Only in a second moment, the chemically linked dye molecules—those that are able to inject photoelectrons into the oxide substrate and to generate a photovoltaic effect—started to degrade depressing the cell power output as well (Fig. 3a). In this respect, the luminescence data represent an early symptom of a degradation process which takes place at the sensitized photoelectrode and can be easily and rapidly detected in intact cells (see ESI).

Regarding the stress tests under light, as long as the stress of the DSC due to irradiation of the cell was not severe (i.e.,: when the UV portion has been filtered off), the phosphorescence intensity remained constant for a rather long time (see inset in Fig. 2b), and so did the cell power output after the initial improvement (not shown). This means that the exposure to the visible light just induced excitation in the dye, and the excess energy was used to both promote charge injection (for those dye molecules chemisorbed onto the TiO_2) and to give rise to light emission (for the fraction of dye molecules physisorbed or free in solution). The addition of the UV component to the light beam impinging on cell C, on the other hand, had a dramatic effect on the phosphorescence intensity, as seen in Fig. 2b, already after 6 h of illumination under 2.5 sun as well as on its electrical performances (see Fig. 3b). The degradation of the electrical performances must be related to the oxidation of the chemisorbed dye molecules by the high-energy holes photogenerated in the valence band of TiO_2, as already postulated by other authors [7–11]. The UV irradiation is also responsible for the steep fall of the cell photopotential (by almost 0.1 V after each of the stress tests reported in Fig. 3b), and that of the cell photocurrent as well. The latter cell parameter decreased only after repeated and even longer exposition to UV-rich radiation. Regarding the phosphorescence data, in analogy with what

already stated about the thermal effects, the exposure to the UV radiation could generate some strong oxydating agents within the electrolyte (e.g., $I^{\bullet}$ from the UV photodissociation of I_2 molecules), which are able to attack the free dye but not the chemisorbed one (it is known that N719 dye gains a certain chemical stability by strongly binding to TiO_2 [8]). Therefore, the removal of the UV component in the radiation source is mandatory for achieving a more effective stability of DSCs under sunlight.

A closer inspection of the photovoltage transients may be helpful for explaining the modification of the DSC performance upon UV irradiation. The faster rising time for the UV-stressed cell could be just a consequence of a light-induced sintering effect (due to the so-called "necking" between the titania nanoparticles [43], or to the increased adhesion of TiO_2 onto the TCO substrate). In fact, this sole effect would improve the DSC performance. On the contrary, we know that both the steady-state photovoltage and the photocurrent decrease after UV irradiation. There is at least another significant change in the photovoltage transient curves, i.e., the faster decay time of the cell photovoltage in the UV-aged cell C, with respect to the reference cell A. For a detailed analysis, the decay curves of such cells have been fitted with four independent exponential decays characterized by four different time constants (k_1, k_2, k_3, and k_4), as shown in ESI. A tentative fit of the two decay curves with the sum of exponentials reveals that in the case of the UV-aged cell, one of the exponential components simply disappears (and it is the one characterized by the smaller kinetic constant), while the other components retain their values except for the obvious redistribution of their relative weights. The lack of this slow-decay component is responsible for the 10-s separation between the two decay curves as already pointed out in the comparison shown in Fig. 4. This is because the photoinjected electrons have a shorter lifetime and recombine with the redox species much faster after UV stress with respect to the non UV-stressed cell. The interpretation of this peculiar behavior of the UV-aged DSC should take into consideration also its spectral and electrical features. The reduction in the luminescence observed for the same cell has been attributed to the UV-induced degradation of the dye free in solution and/or physisorbed to both TiO_2 and TCO. These last dye molecules could act as passivating plugs on top of the recombination sites. As DSCs are devices driven by the transport of the majority carrier and they become operative when the semiconducting anode undergoes a tremendous increase of electron population upon illumination, it is crucial that such photoinjected electrons do not recombine before reaching the external circuit. Therefore, in the balance between favorable and negative effects of UV irradiation, the creation of more recombination centers under UV is the most deleterious consequence of such light-soaking treatment, and thus should be avoided as much as possible.

5 Conclusions

In-situ luminescence spectra and transient photovoltage measurements taken on fresh, stressed, and/or degraded DSCs have shown some significant and reproducible differences among each other. The emission spectra remain unchanged in intensity as long as the stress test has brought no or negligible degradation to the long-life power output of the device, such as for cells exposed to UV-filtered white light at 1 sun (and even at 2.5 sun for short time). On the contrary, stress tests promoting a degradation of the solar cell power output on the long run, such as thermal cycles up to 80 °C and back to room T, or the irradiation under a Xe lamp without any UV filter, are responsible for a relatively rapid decrease of the cell phosphorescence intensity. As the photo-emission decrease always precedes the degradation in the solar cell power output, this can be taken as a symptom of incipient DSC's instability and failure. The explanation for this effect is in the faster degradation of such dye molecules, detected via the phosphorescence measurements, with a failed or a weak bond to the TiO_2 electrode. Regarding the photovoltage transient experiments, UV-aged cells have shown faster rise time and faster decay time, besides a lower steady-state photovoltage under illumination. The shorter decay time is a consequence of a higher recombination rate of the injected electrons, which is more evident in the long-time tail of the decay curve. So far it, therefore, appears that the fresher the DSC, the longer its photovoltage decay time is. The investigations in our lab also suggest that the amount of electrons that can be extracted by the TiO_2, calculated according to the literature [44], change before and after any aging treatment. Stress tests under reverse bias [45] on robust master plates having already passed long durability tests outdoor [46] are presently ongoing and will be reported in further studies, where the efficiency of the rinsing process after the dye soaking of the TiO_2/TCO electrode also will be carefully investigated.

Acknowledgments M. G. thanks the CSGI for the partial financial support. The authors wish to thank both Referees for their precious suggestions that increased the readability of the manuscript.

References

1. O'Regan B, Grätzel M (1991) Nature 353:737
2. Ashgar MI, Miettunen K, Halme J, Vahermaa P, Toivola M, Aitola K, Lund P (2010) Energy Environ Sci 3:418

3. Nazeeruddin MK, De Angelis F, Fantacci S, Selloni A, Viscardi G, Liska P, Ito S, Takeru B, Grätzel M (2005) J Am Chem Soc 127:16835
4. Gao F, Wang Y, Shi D, Zhang J, Wang M, Jing X, Humphry-Baker R, Wang P, Zakeeruddin SM, Grätzel M (2008) J Am Chem Soc 130:10720
5. Bessho T, Zakeeruddin SM, Yeh CY, Wei-Guang Diau E, Grätzel M (2010) Angewandte Chem Int Ed 49:6646
6. Yella A, Lee HW, Tsao HN, Yi CY, Chandiran AK, Nazeeruddin MK, Diau EWG, Yeh CY, Zakeeruddin SM, Grätzel M (2011) Science 334:629
7. Hinsch A, Kroon JM, Kern R, Uhlendorf I, Holzbock J, Meyer A, Ferber J (2001) Progr Photovolt Res Appl 9:425
8. Grünwald R, Tributsch H (1997) J Phys Chem B 101:2564
9. Kay A, Grätzel M (1996) Sol Energy Mater Sol Cells 44:99
10. Nazeeruddin MK, Kay A, Rodicio I, Humphry-Baker R, Müller E, Liska P, Vlachopoulos, Grätzel M (1993) J Am Chem Soc 115:6382
11. Ikegami M, Suzuki J, Teshima K, Kawaraya M, Miyakasa T (2009) Sol Energy Mater Sol Cells 93:836
12. Wang P, Zakeeruddin SM, Moser JE, Nazeeruddin MK, Sekiguchi T, Grätzel M (2003) Nature Mater 2:402
13. Toivola M, Peltokorpi L, Halme J, Lund P (2007) Sol Energy Mater Sol Cells 91:1733
14. Sommeling PM, Späth M, Smit HJP, Bakker NJ, Kroon JM (2004) J Photochem Photobiol A 164:137
15. Matsui H, Okada K, Kitamura T, Tanabe N (2009) Sol Energy Mater Sol Cells 93:1110
16. Grätzel M (2006) Comptes Rendus Chimie 9:578
17. Harikisun R, Desilvestro H (2011) Sol Energy 85:1179
18. Kato N, Higuchi K, Tanaka H, Nakajima J, Sano T, Toyoda T (2011) Sol Energy Mater Sol Cells 95:301
19. Pettersson H, Gruszecki T (2001) Sol Energy Mater Sol Cells 70:203
20. Pettersson H, Gruszecki T, Johansson LH, Johander P (2003) Sol Energy Mater Sol Cells 77:405
21. Hagfeldt A, Boschloo G, Sun L, Kloo L, Pettersson H (2010) Chem Rev 110:6595
22. Figgenmeier E, Hagfeldt A (2004) Int J Photoenergy 6:127 and references therein
23. International Electrotechnical Commission (IEC) (2008) Standards, document number 61646: thin-film terrestrial photovoltaic (PV) modules—Design qualification and type approval
24. International Electrotechnical Commission (IEC) (2002) Standards, document number 60721-2-1: classification of environmental conditions—Part 2–1: Environmental conditions appearing in nature—Temperature and humidity
25. Kato N, Takeda Y, Higuchi K, Takeichi A, Sudo E, Tanaka H, Motohiro T, Sano T, Toyoda T (2009) Sol Energy Mater Sol Cells 93:893
26. Wang Q, Moser JE, Grätzel M (2005) J Phys Chem B 109:14945
27. Toivola M, Halme J, Peltokorpi L, Lund P (2009) Int J Photoenergy 786429. doi:10.1155/2009/786429
28. Paulsson H, Kloo L, Hagfeldt A, Boschloo G (2006) J Electroanal Chem 586:56
29. Schlichthörl G, Huang SY, Sprqague J, Frank AJ (1997) J Phys Chem B 101:8141
30. Estrada W, Andersson AM, Granqvist CG, Gorenstein A, Decker F (1991) J Mater Res 6:1715
31. Agrell HG, Lindgren J, Hagfeldt A (2003) Sol Energy 75:169
32. Sirimanne PM, Jeranko T, Bogdanoff P, Fiechter S, Tributsch H (2003) Semicond Sci Technol 18:708
33. Hara K, Wang ZS, Cui Y, Furube A, Koumura N (2009) Energy Environ Sci 2:1109
34. Walker AB, Peter LM, Lobato K, Cameron PJ (2006) J Phys Chem B 110:25504
35. Cerdeira F, Torriani I, Motisuke P, Lemos V, Decker F (1988) Appl Phys A 46:107–112
36. Abramovich M, Brasil MJP, Decker F, Moro J, Motisuke P (1985) J Solid State Chem 59:1
37. Smestad G (1994) Sol Energy Mater Sol Cells 32:273
38. Lee CY, Hupp JT (2010) Langmuir 26:3760
39. Bräm O, Canizzo A, Chergui M (2012) Phys Chem Chem Phys 14:7934
40. Bräm O, Messina F, El-Zohry AM, Canizzo A, Chergui M (2012) Chem Phys 393:51
41. Lewis LN, Spivak JL, Gasaway S, Williams ED, Guy JY, Manivannan V, Siclovan OP (2006) Sol Energy Mater Sol Cells 90:1041
42. Boschloo G, Hagfeldt A (2009) Acc Chem Res 42:1819
43. Gregg BA, Chen S, Ferrere S (2003) J Phys Chem B 107:3019
44. Duffy NW, Peter LM, Rajapakse RMG, Wijayantha KGU (2000) J Phys Chem B 104:8916
45. Mastroianni S, Lembo A, Brown TM, Reale A, Di Carlo A (2012) Chem Phys Chem 13:2964. doi:10.1002/cphc.201200229
46. Mastroianni S, Lanuti A, Penna S, Brown TM, Reale A, Di Carlo A, Decker F (2012) Chem Phys Chem 13:2925. doi:10.1002/cphc.201200110